JMEPEG (2009) 18:1230–1240
DOI: 10.1007/s11665-009-9362-5

1059-9495/$19.00

Processing of Aluminum-Graphite Particulate Metal Matrix Composites by Advanced Shear Technology

N. Barekar, S. Tzamtzis, B.K. Dhindaw, J. Patel, N. Hari Babu, and Z. Fan

(Submitted August 12, 2008)

To extend the possibilities of using aluminum/graphite composites as structural materials, a novel process is developed. The conventional methods often produce agglomerated structures exhibiting lower strength and ductility. To overcome the cohesive force of the agglomerates, a melt conditioned high-pressure die casting (MC-HPDC) process innovatively adapts the well-established, high-shear dispersive mixing action of a twin screw mechanism. The distribution of particles and properties of composites are quantitatively evaluated. The adopted rheo process significantly improved the distribution of the reinforcement in the matrix with a strong interfacial bond between the two. A good combination of improved ultimate tensile strength (UTS) and tensile elongation (ε) is obtained compared with composites produced by conventional processes.

Keywords Agglomerates, Intensive shearing, Mechanical properties, Metal matrix composites, Particle distribution

1. Introduction

The need for engineering materials with the technological importance for the areas of air and land vehicles has led to a rapid development of composite materials. Composite materials have an edge over monolithic materials because of their superior properties such as high specific strength and stiffness, increased wear resistance, enhanced temperature performance together with better thermal and mechanical fatigue and creep resistance (Ref 1, 2). Metal matrix composites (MMCs) are one of the important innovations in the development of advanced materials. Among the various matrix materials available, aluminum and its alloys are widely used in the fabrication of MMCs and have reached the industrial production stage. The emphasis has been given on developing affordable Al-based MMCs with various hard and soft reinforcements (SiC, Al_2O_3, zircon, graphite, and mica) because of the likely possibilities of these combinations in forming highly desirable composites (Ref 3-5).

Graphite, in the form of fibers or particulates, has long been recognized as a high-strength, low-density material. Aluminum graphite particulate MMCs produced by solidification techniques represent a class of inexpensive tailor-made materials for a variety of engineering applications such as automotive components (Ref 6, 7), bushes, and bearings (Ref 8, 9). Their uses are being explored in view of their superior technological properties such as the low coefficient of friction (Ref 10, 11), low wear rate (Ref 11-13), superior gall resistance (Ref 11, 14), high seizure resistance (Ref 11, 15), high damping capacity (Ref 16, 17) and good machinability (Ref 18, 19).

Several processes involving incorporating graphite particles in aluminum-base alloy to produce particulate composites have been developed (Ref 20-23). While powder metallurgy (Ref 24) is a powerful method to produce such composites in mass scale production of small components, the liquid metallurgy techniques are attracting much attention because of their inherent production advantages (Ref 4, 5). The most economical production of such composites is by stir casting; nevertheless, this is associated with some problems arising mainly from the apparent non-wettability of graphite by liquid aluminum alloys (Ref 25-27) and density differences between the two materials (Ref 28). As a result, the introduction and retention of graphite particles in molten aluminum is extremely difficult.

Several investigations have been documented to improve the wettability between the two components by special treatment of both, the particles and melt (Ref 29, 30). A considerable amount of studies have been carried out in the area of development of processes, the characterization of the structure, and properties of these materials (Ref 24, 31-35). Earlier it has been reported that the production method has a strong influence on the mechanical and tribological properties of composites through its effects on the matrix grain size, porosity, the distribution of graphite particles, and the interfacial properties of the Al/graphite couple (Ref 36-39). Improvements in tribological properties are, however, accompanied by a decrease in the strength and ductility of these composites (Ref 40). In order to explore the possibilities of using Al/graphite composites as structural materials, mechanical properties need to be enhanced by controlling the nature of the distribution of the graphite particles and the interface that exists between the graphite and the matrix.

Although considerable effort has been made to study this interface and its effects on properties (Ref 39), very little information is available on the reinforcement distribution within the matrix. Despite the growing popularity of these cast metal-graphite particle composites, no study on characterization of reinforcement distribution influenced by processing parameters has been reported as yet. Defects such as clusters,

N. Barekar and **B.K. Dhindaw**, Department of Metallurgical and Materials Engineering, Indian Institute of Technology, Kharagpur 721302, India; and **N. Barekar, S. Tzamtzis, J. Patel, N. Hari Babu,** and **Z. Fan**, BCAST (Brunel Centre for Advanced Solidification Technology), Brunel University, Uxbridge, Middlesex UB8 3PH, UK. Contact e-mail: dhindaw@metal.iitkgp.ernet.in.

agglomerates, and segregation of graphite particles play a dominant role in accelerating the fracture process (Ref 41). An inhomogeneous distribution of the particles, inadequate bonding between the metal and graphite particles, and formation of porosity at the graphite/matrix interface could be reduced to some extent by using pressure diecasting (Ref 41-43). In order to obtain a homogeneous distribution of reinforcement particles in the matrix, current processing methods require to be revised.

In view of the above mentioned problems, this study was undertaken to produce advanced Al/graphite composites with high-quality microstructures characterized by a uniform distribution of the reinforcement throughout the whole sample and good mechanical properties of the final product. The key idea is to apply sufficient shear stress (τ) on particle clusters embedded in the liquid metal to overcome the average cohesive force or the tensile strength of the cluster. A new rheo process has been developed at Brunel Centre for Advanced Solidification Technology (BCAST), Brunel University, by utilizing the MCAST (Melt Conditioning by Advanced Shear Technology) process, in which the liquid undergoes a high-shear stress and a high intensity of turbulence inside a specially designed twin-screw machine (Ref 44, 45). The effect of processing parameters on the reinforcement distribution has also been examined with the purpose of optimizing the process parameters to yield components of high integrity. The variation of inhomogeneity caused by process variables has been quantitatively analyzed. The experimental results of novel melt-conditioned high-pressure die cast (MC-HPDC) Al alloy composites are compared with conventional high-pressure die casting (HPDC) samples. The adopted rheo process clearly demonstrates a significant improvement in the distribution of the reinforcement in the matrix with a good combination of improved ultimate tensile strength (UTS) and tensile elongation (ε).

2. Experimental Procedures

2.1 Processing

Commercially available HPDC Al-alloy LM24 (USA designation A380) was used as the matrix material for this study. The alloy LM24 (composition shown in Table 1) has an excellent combination of mechanical properties in the cast condition. Interfacial reactions with the reinforcement under a prolonged contact time at elevated temperature is avoided due to the high Si content (Ref 46, 47). A properly cleaned ingot was melted in a cylindrical crucible inside a top-loaded resistance furnace at 650 °C. Uncoated but pre-heat treated (heated at 400 °C for approximately 1 h (Ref 21)) synthetic graphite powder (particle size $\leq$20 μm) was used as the reinforcement.

The novel process for synthesizing Al/graphite composite consists of two steps:

1. distributive mixing;
2. dispersive mixing under intensive shearing.

Table 1 Chemical composition (wt.%) of the Al-alloy used in this study

Cu	Mg	Si	Fe	Mn	Ni	Zn	Pb	Sn	Ti	Al
3.37	0.13	8.54	1.20	0.19	0.04	1.36	0.07	0.03	0.04	REM

2.1.1 Distributive Mixing. Distributive mixing employs conventional mechanical stirring (Ref 4, 5) to pre-mix the Al alloy with graphite particles. The mixing equipment (Fig. 1) consisted of a driving motor to create the torque on the impeller, a lifting mechanism for the rotation drive unit and stirrer assembly, and a transfer tube for introducing the graphite powder into the melt. To ensure a uniform distribution, the impeller was designed to have a d/D ratio equal to 0.4 and a w/d ratio equal to 0.35 (Ref 48) where D is the inner diameter of the crucible, d is the diameter of the impeller, and w is the width of the impeller. A four-bladed stainless steel impeller was coated with boron nitride to prevent a reaction with molten aluminum. A controlled argon atmosphere was maintained inside the furnace throughout the whole experiment to prevent melt oxidation. The graphite particles (5 vol.% $\cong$ 3.5 wt.%) were transferred slowly and continuously into the melt which was mechanically stirred at 600-800 rpm. After all the graphite powder was introduced successfully into the liquid metal, the composite mixture was allowed to solidify in the crucible and subsequently reheated to the preset melting temperature. It was then restirred for 2 min at approximately 400 rpm and was transferred into a 280-tonne cold chamber HPDC machine (LK Machinery, Hong Kong) to produce standard tensile test samples. For all the experiments in this study, the die temperature was kept at 220 °C. The samples cast in this conventional method are referred as 'HPDC' samples.

2.1.2 Dispersive Mixing. The distributive mixing stage is important as a means to incorporate the graphite particles and to distribute them in the melt. The degree of mixing in conventional mechanical stirring is governed by the momentum transfer from the position of the stirrer to the particles located away from the stirrer position (Ref 49, 50). Due to a diminishing velocity gradient from the center to the wall within the liquid, the degree of mixing is limited. A lack of sufficient shear force in distributive mixing results in agglomerates in relatively stagnant zones (e.g., near crucible walls).

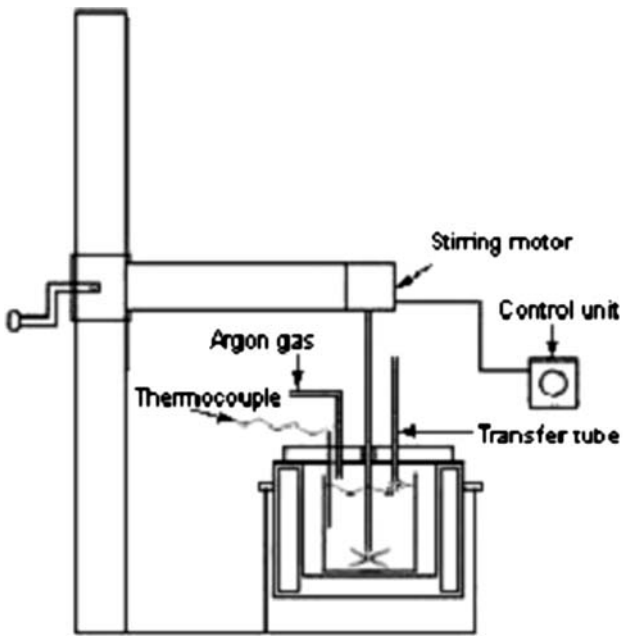

Fig. 1 Schematic diagram of the distributive mixing equipment

In order to break up the agglomerates, it is important to apply an adequate shear stress which overcomes the average cohesive force or tensile strength of the clusters (Ref 51, 52).

The process of dispersive mixing under intensive shearing innovatively adopts a high-shear dispersive mixing action of the twin-screw mechanism (Ref 44) to the task of overcoming the cohesive force of agglomerates. The twin-screw mechanism used for the MCAST process consists of a pair of co-rotating, fully intermeshing, and self-wiping screws. The screws have specially designed profiles (Fig. 2) which result in high-shear rate and high intensity of turbulence. The screws and barrel are made from a special material to avoid a reaction with molten aluminum. A more detailed description of fluid flow in the MCAST machine can be found in Ref 45, 53. The basic function of the twin screws is to break up the agglomerates and clusters embedded in the liquid melt under a high-shear stress and disperse the particles uniformly under the high intensity of turbulence.

The pre-mixed composite mixture after distributive mixing as explained above was fed into the MCAST machine (Fig. 3). The MCAST machine was operated above liquidus temperature in the range between 600 and 620 °C. The rotation speed of the twin screws was 800 rpm and the shearing time was varied between 60 and 240 s. After the predetermined shearing time, the high quality composite slurry was transferred to the HPDC machine with a 280-tonne clamping force, to produce standard tensile test samples. These composites are referred as 'MC-HPDC'. The die used for casting test samples had four cavities, of which two were for tensile test samples and two were for fatigue test samples. The dimensions of the tensile test samples are 6 mm in gauge diameter, 60 mm in gauge length, and 150 mm in total length. The data from the fatigue tests will be the subject of a later report.

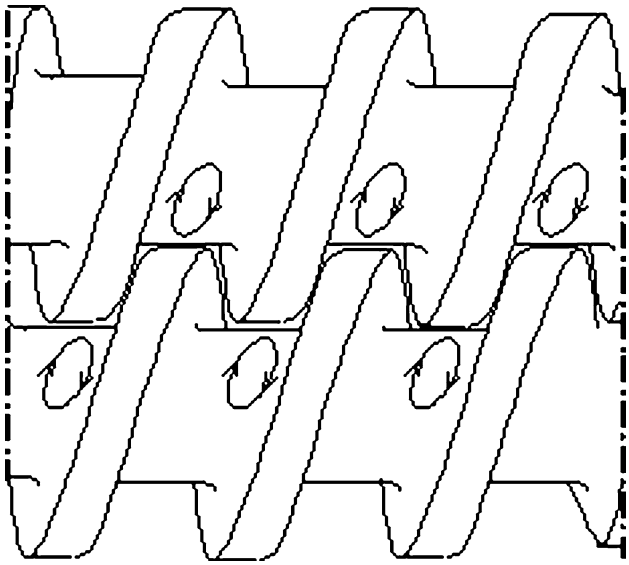

Fig. 2 Schematic showing the profile of the twin screws

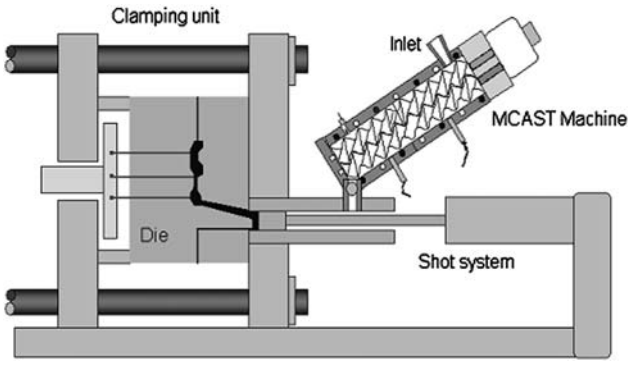

Fig. 3 Schematic illustration of the MC-HPDC process

2.2 Metallographic Characterization and Mechanical Properties

Specimens for microstructural characterization were cut from different positions of the final castings. The microstructures were examined by optical microscopy (OM), using a Carl Zeiss Axioskop 2 MAT microscope, and scanning electron microscopy (SEM), using a Zeiss Supra 35VP FEG microscope equipped with energy dispersive x-ray (EDX), Oxford Instruments Inca, and data were ZAF corrected. The specimens for microscopical observations were prepared by the standard technique of grinding with SiC abrasive papers and polishing with a diamond suspension solution. For a quantitative analysis of the distribution of the reinforcement particles in the MMC, an area count method was used (Ref 54, 55). The area count method effectively detects pronounced changes in the MMC microstructure and then the observed distribution can be compared with some theoretical models.

The area to be studied was divided into 25 contiguous quadrats with a quadrat side of 54 μm (168 pixels) at 200× magnification. The quadrat size was approximately twice the size of the mean area per particle (Ref 56). The area count method was performed on 40 images of each specimen. To minimize the edge effects, particles only inside and in contact with the left and bottom side of each quadrat were counted. Problems associated with image analysis could result in errors such as (i) pronounced clustering and touching of graphite particles in a cast MMC leads to identifying some of them as one particle as it is based on gray color differences among the features; (ii) distinguishing very small graphite particles from artifacts, such as intermetallic particles and pores. These problems can be minimized by carefully defining the size range (<20 μm) for measurement of the particles and increasing the magnification.

The number of particles, N_q, was measured and the degree of asymmetry of a statistical distribution around its mean can be quantified by its skewness, β, which is defined by:

$$\beta = \frac{q}{(q-1)(q-2)} \sum \left[\frac{N_{qi} - N_q^{\text{mean}}}{\sigma} \right]^3 \qquad \text{(Eq 1)}$$

where q is the total number of quadrats studied, N_{qi} is the number of graphite particles in the ith quadrat ($i = 1,2,\ldots,q$), N_q^{mean} is the mean number of graphite particles per quadrat, and σ is the standard deviation of the N_q distribution. According to the microstructural observations, an increase in β indicates an increase in graphite clustering.

In mathematical terms a theoretically random, a spatial, and a clustered spatial distribution of particles can be expressed by a Poisson distribution, a binomial distribution, and a negative binomial distribution respectively (Ref 57). The dispersion coefficient (DC) is defined as the relation between the square of

the experimentally determined standard deviation (*S*) to the experimental average value (*N*) of the counted number of particles.

$$DC = \frac{S^2}{N} \quad \text{(Eq 2)}$$

DC equals 1 for a Poisson distribution and is an indication of the randomness of the particle dispersion. A value smaller than 1 indicates that an observed distribution is more homogeneous than random (Ref 55). The major source of divergence from the Poisson distribution as indicated by a high DC is the presence of clusters and agglomerates.

The mechanical property tests were carried out using a universal materials testing machine (Instron® 5569) at a cross head speed of 2 mm/min. Dry sliding abrasion wear tests were carried out using a pin on disk wear test apparatus. In brief, the test consisted of holding a cylindrical sample (8-mm diameter) against a rotating SiC paper disc (Struers, 500 grit, HV 30-800) under 1-kg load. A wear track diameter of 128 mm provided a sliding velocity of 1 m/s. Wear loss (mm^3) were calculated from the length of wear test pin lost at intervals of 200-m sliding distance. The length of pin lost during the test was measured using a vernier caliper accurate to 0.03 mm. For the purpose of comparison of mechanical properties, the base alloy (LM24) was also sheared in the MCAST machine using similar superheat temperatures and processing conditions as described above and shaped to produce standard tensile test samples by HPDC.

3. Results and Discussion

3.1 General Microstructures

Figure 4 shows typical optical microstructures of LM24-5 vol.% graphite composites from (a) conventional HPDC and (b) MC-HPDC. In the microstructure of the conventional HPDC composite, agglomerates of the reinforcement particles are clearly visible, whereas the MC-HPDC composite sample shows a more uniform distribution of the reinforcement. During the distributive mixing, the rotation of the stirrer generates a vortex through which the graphite particles are drawn into the melt. The force provided by stirring the melt with a mechanical stirrer helps to overcome the surface energy barriers due to poor wettability of graphite by Al alloy. Once the particles are transferred into the liquid, the distribution is strongly affected by certain flow transitions. The axial flow causes lifting of particles due to momentum transfer and radial flow prevents particle settling. A high and local shear force is exerted on the agglomerates of the bulk cohesive graphite powder. The maximum force on a particle cluster rotating in a shear flow in the vicinity of a stirrer is given by (Ref 49):

$$F = 6\pi\eta\alpha^2\dot{\gamma} \quad \text{(Eq 3)}$$

where α is the radius of each primary particle in the cluster, η is the viscosity, and $\dot{\gamma}$ is the shear rate in the surrounding liquid medium. A lack of sufficient hydrodynamic forces due to a variation in the velocity gradients results in accumulation of the aggregates in relatively stagnant zones where they survive the shear forces of mixing. These agglomerates are not transported back into the high-shear regions and finally find their way as clusters into the cast structures. Thus mixing is limited for the clusters located away from the impeller, resulting in the characteristic microstructure seen in Fig. 4(a).

As stated before intensive shearing is required to break down the agglomerates into individual particles by applying a shear stress that will overcome the average cohesive force or the tensile strength of cluster. According to Kendall's model (Ref 52), the strength of an agglomerate is given by:

$$T = 11.30\frac{\phi^4\Gamma_c{}^{5/6}\Gamma^{1/6}}{\sqrt{l_f d}} \quad \text{(Eq 4)}$$

where ϕ is the volume fraction of particles, Γ_c and Γ are the fracture surface energy and equilibrium surface energy, respectively, and l_f is the flaw size in the cluster. Previously it

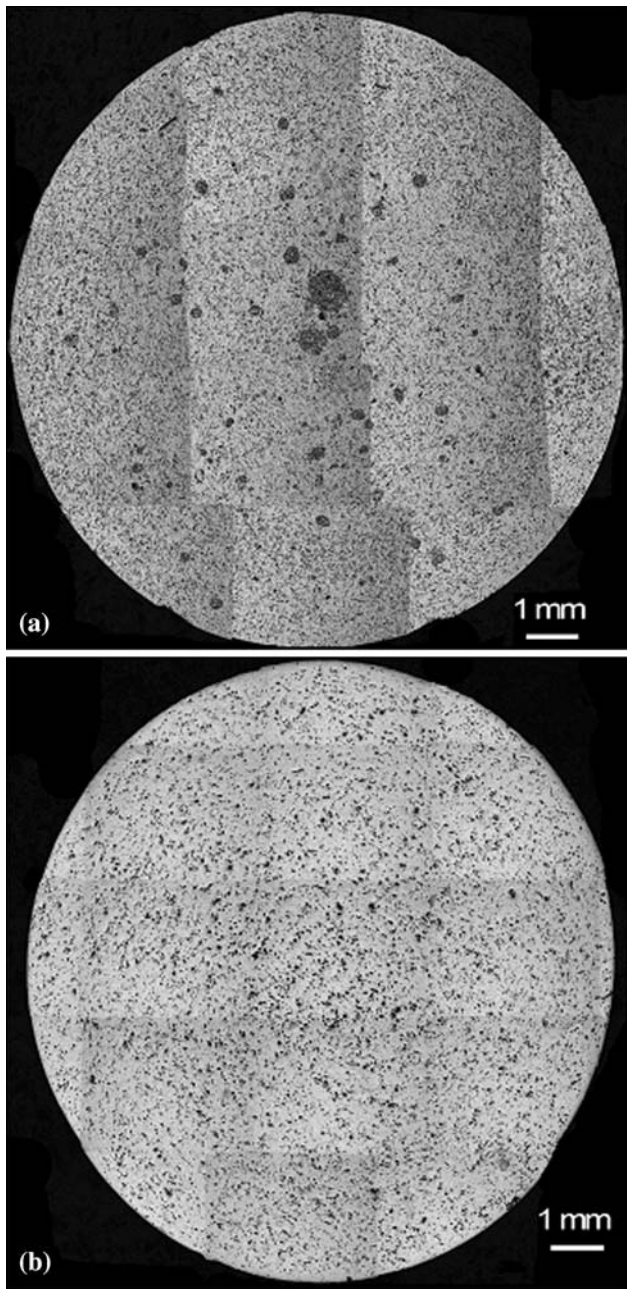

Fig. 4 Typical optical microstructures taken from LM24-5% graphite composite samples (a) conventional HPDC, (b) MC-HPDC

has been reported that the tensile strength of cohesive particles is about 300 kPa (Ref 58). According to this, the application of a high-shear stress is necessary in order to break down the clusters. This can be achieved in rheo process using the MCAST machine in which fluid flow is characterized by a cyclic variation of a high-shear rate, high intensity of turbulence, and positive displacement pumping action. The fluid moves in the periphery of the screws in a 'figure of 8' motion moving from one pitch to the next. In the continuous flow field, the fluid undergoes cycling stretching, folding, and reorienting processes. The fluid flow inside the MCAST machine is shown schematically in Fig. 5.

Based on the fluid flow, the shear rate between the screws and the barrel in the MCAST machine can be given by (Ref 59):

$$\tau = \eta \pi N \left(\frac{D}{G} - 2 \right) \quad \text{(Eq 5)}$$

where η is the viscosity, N is the rotation speed of the screws, D is the outer diameter of the screws, and G is the gap between the screw flight and the barrel surface.

Depending upon the viscosity and rotational speed, an adequate shear rate can be applied in MCAST machine to overcome the cohesive force of agglomerates given by Eq 4. The combination of the fluid dynamics briefly described above and an enormous amount of ever changing interfacial contacting surface compared to conventional stirrers contribute to the high-shear dispersive mixing action of the twin screws. The hydrodynamic stresses developed are capable of breaking down the agglomerates of graphite particles and result in a more homogeneous microstructure throughout the cast component as shown in Fig. 6. Image analysis on microstructures of LM24-5% graphite has shown the reinforcement volume fractions to be $4.93 \pm 1.26\%$. Density of the MC-HPDC composite sample was measured using Archimedes' principle as discussed in Ref 60 and rule of mixtures (ROMs) (Ref 1) and found to be 2.58 ± 0.06 and 2.66 g/cm^3, respectively, indicating negligible porosity.

3.2 Effect of processing parameters on degree of homogeneity

Experiments were carried out to investigate the effect of processing parameters such as shearing time (60-240 s), shearing temperature (600-620 °C) and shearing speed (400-800 rpm). The range of processing parameters was selected so as to apply sufficient hydrodynamic force and to maintain optimum fluidity for casting. The calculated skewness, an indicative of the degree of homogeneity is plotted as a function of processing parameters in Fig. 7.

The calculated skewness for the conventional HPDC sample is significantly higher than that observed for the MC-HPDC samples representing the clustering tendency. At a shearing time of 0 s corresponding to the HPDC sample, the skewness value is 2.45. With MC-HPDC composite material, β ranges from 1.62, for a sample processed at 610 °C for 60 s, to 0.19 for a sample processed at 610 °C for 180 s. The skewness value decreased with shearing time up to 180 s and then increased at 240 s. An increased shearing time dissociates the inter-aggregate bonds but can also increase the frequency of multi-particle interactions resulting in the formation of new agglomerates which impair the mixture quality (Ref 51, 61).

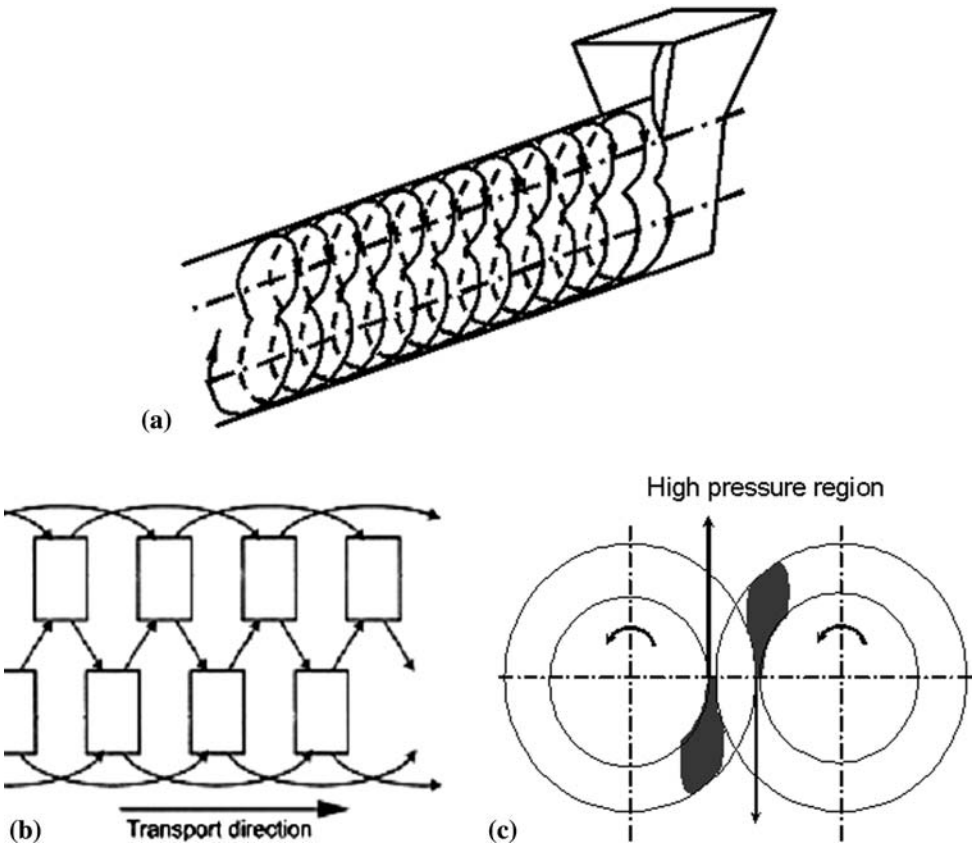

Fig. 5 Fluid flow pattern in MCAST machine (a) 'figure of 8' motion of the slurry, (b) positive displacement of slurry, (c) high-shear zones

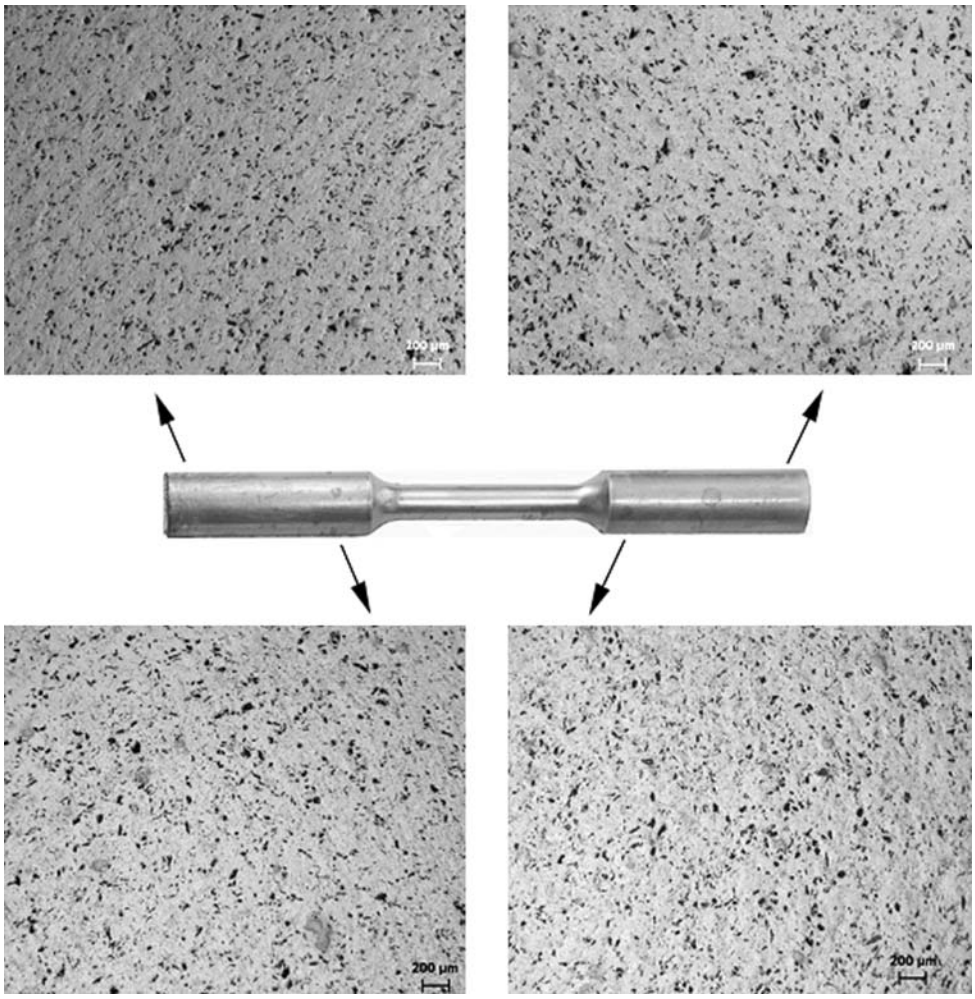

Fig. 6 Microstructures of cross section at different regions of LM24-5% graphite MC-HPDC tensile sample

Figure 7 also indicates that increasing the processing temperature from 600 to 620 °C enhances dispersion of the reinforcement. The apparent viscosity decreases as the temperature increases which in turn decreases the shear stress (τ) as also predicted by Eq 5. The decrease in shear stress prevents flocculation, the process that reduces the number of particles due to collision between the particles under dynamic shear conditions. To maintain the dispersion and to improve the fluidity of the Al/graphite slurry and to die cast the sheared slurry into required shapes, it is necessary to work above liquidus temperature of alloy. HPDC experiments were also carried out above liquidus temperature (approximately 630 °C). The calculated DC for conventional HPDC is 9.79 ± 0.27 and the corresponding values for MC-HPDC samples ranges from 0.23 ± 0.21, for a sample processed at 610 °C and 180 s, to 4.12 ± 0.20 for a sample processed at 600 °C and 60 s. The decrease observed in the value of DC for MC-HPDC clearly suggests the structural homogeneity.

Figure 8 presents the variation in DC as a function of shearing speed, and value corresponding to 0 rpm stands for HPDC sample. When the screw rotational speed is increased from 400 to 600 rpm, the DC during the shearing process decreased from 1.79 ± 0.20 to 0.43 ± 0.20 for LM24-5%

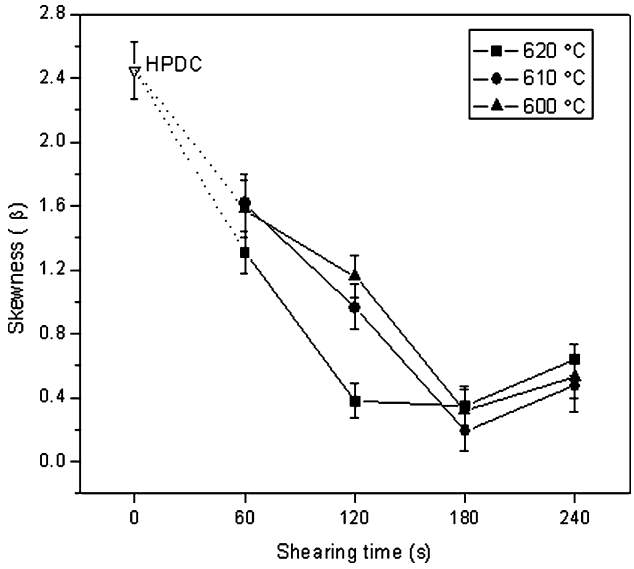

Fig. 7 Skewness (β) as a function of shearing time at a rotation speed of 800 rpm for MC-HPDC samples

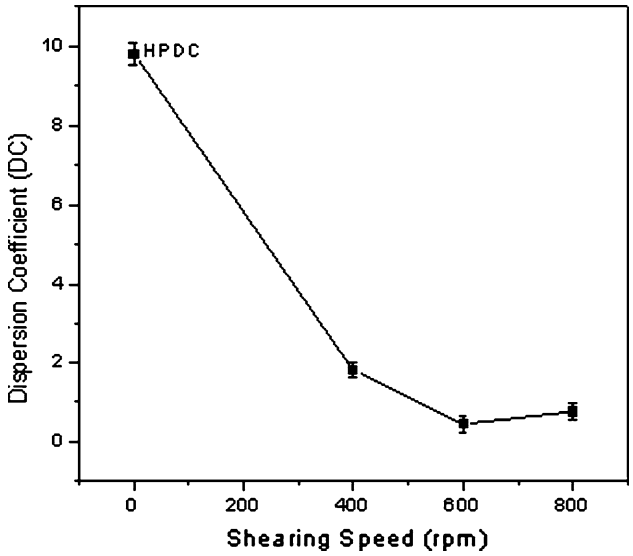

Fig. 8 Dispersion Coefficient as a function of shearing speed at 610 °C and 120 s

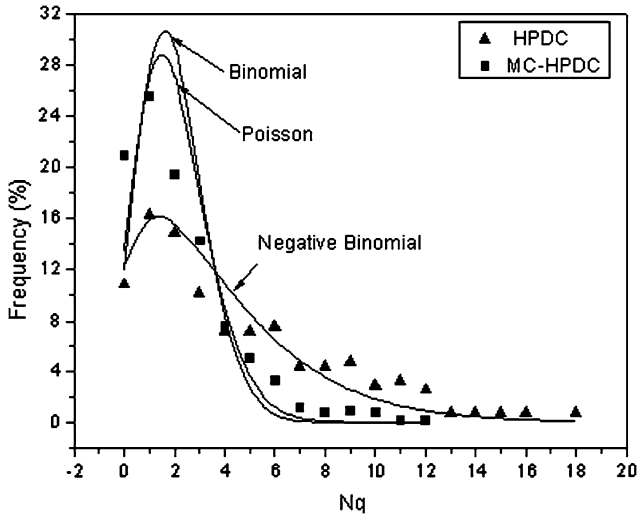

Fig. 9 Theoretical distribution curves and experimental results (symbols) from an area count analysis for LM24-5 vol.% graphite samples

graphite composite. The decrease in DC with an increase in shearing speed is because of the increase in shear rate with rotational speed. An increase in shear rate breaks up the agglomerates by overcoming the cohesive forces which hold them together. Under a high-shear stress and turbulent conditions, the melt penetrates into the clusters and disperses the individual particles within the cluster, resulting in a more uniform distribution. The shear stress (τ) predicted by Eq 5 also suggests that an increase in rotational speed of the screws, increases the applied shear stress and contributes to homogeneity of the reinforcement distribution. The increase in dispersion coefficient for a sample processed at 800 rpm may be associated with flocculation because of multi-particles interaction under increased dynamic shear conditions.

The experimental results from the area count analysis can be compared with theoretical distribution curves in absolute terms (Ref 54). Figure 9 indicates that the observed distribution for composite made by the conventional HPDC process follows a clustered distribution expressed by a negative binomial curve, whereas the corresponding distribution for the novel MC-HPDC composite is closer to both the Poisson and the binomial distributions compared to the negative binomial distribution, indicating a more uniform distribution.

Owing to pinhole porosity and polishing defects, observation under the optical microscope fails to distinguish between graphite particles and micropores in the composite materials (Ref 31). To ascertain the graphite distribution in the matrix and the surface details of composite materials, scanning electron microscopy (SEM) is a powerful tool. SEMs have very high resolving power coupled with high depth of focus, offering the best advantage for assessing the microstructure. Figure 10 shows the micrograph of MC-HPDC Al/graphite composite processed at 610 °C and 800 rpm for 180 s, confirming the uniform distribution of graphite particles.

3.3 Interfacial Analysis

A strong bond between the reinforcement and matrix helps in the load transfer from the latter to the former. As a result, fracture takes place in the composite via the reinforcement and

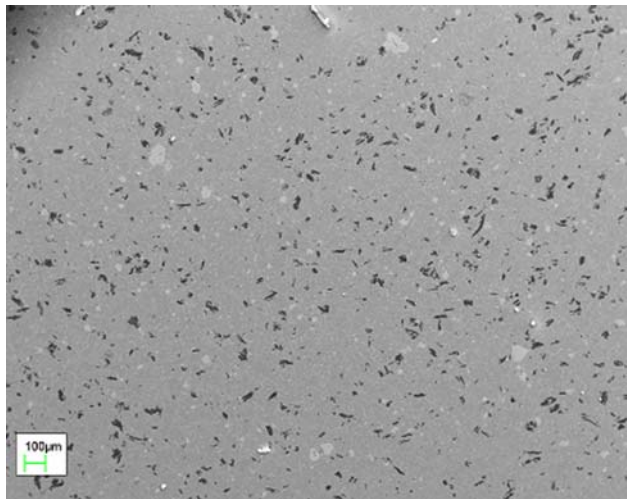

Fig. 10 Scanning electron micrograph showing a uniform distribution of graphite particles (dark in contrast)

not along the interface (Ref 1, 2). Although the graphite is a non-load bearing constituent, a strong particle/matrix interface helps graphite particles embed themselves into the matrix properly, improving the fracture resistance. An improvement in interfacial bonding between the graphite and aluminum matrix under pressure during solidification has been reported (Ref 43). In this investigation, fractographic features of a MC-HPDC LM24-5 vol.% graphite sample processed at 610 °C and 800 rpm for 180 s, after tensile testing have been observed as shown in Fig. 11.

Good bonding between the graphite particle and the matrix is evident. There is no sign of void formation or extensive separation at the particle-matrix interface. The particles are well embedded in the matrix and the fracture shows ductile behavior as river patterns are quite prominent. Scanning electron microscopy (Fig. 12) of MC-HPDC sample of the same composite also supports the fact that the interface is clean and sharp without any evidence for the formation of aluminum

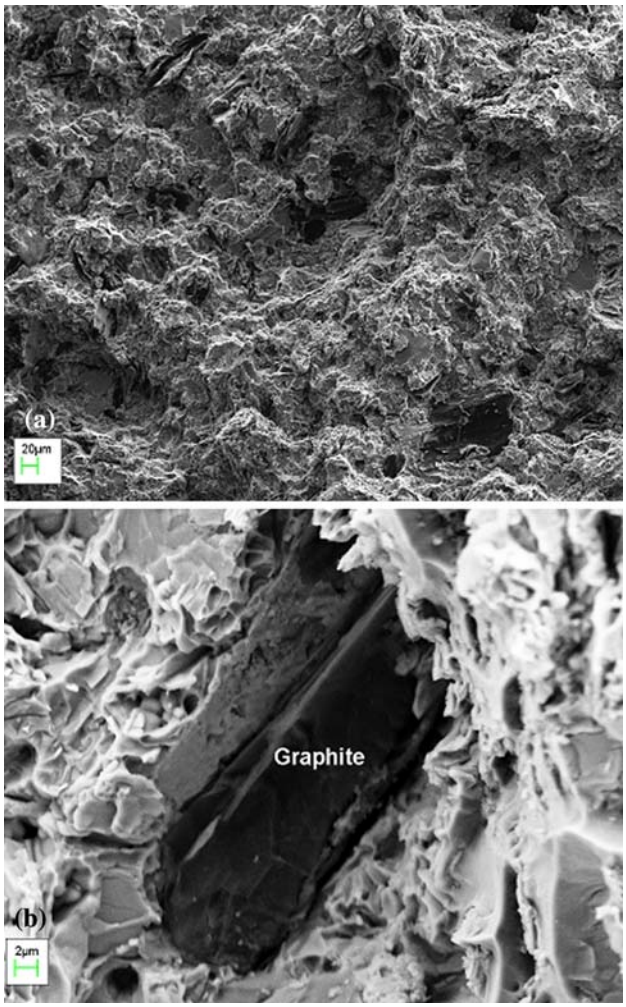

Fig. 11 Fractographs of MC-HPDC Aluminum-graphite composite showing (a) ductile failure, (b) improved interfacial bonding

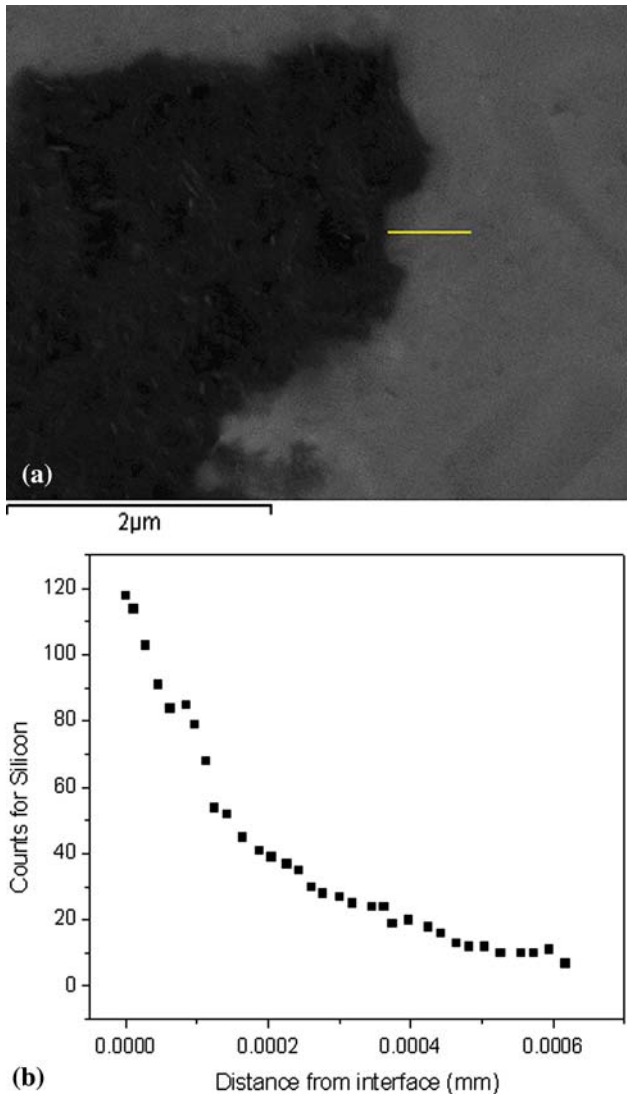

Fig. 12 Scanning electron micrograph with EDX line analysis of a MC-HPDC composite sample showing a clean interface between a graphite particle and the aluminum matrix

carbide at the interface. Graphite can form aluminum carbide when it comes into contact with molten aluminum alloys at temperatures exceeding 627 °C and long contact time (Ref 29, 30, 39, 62, 63). One possible way to limit carbide formation is to alloy aluminum with elements very similar to carbon and change the interaction character on the interfacial boundary (Ref 64). Silicon is one such element. The addition of Si (from 7 to 10%) decreases carbon solubility in Al because a SiC layer or segregated Si may act as a diffusion barrier for C diffusion which reduces the reaction rate between C and Al which finally eliminates the formation of Al_4C_3 (Ref 46, 47). Further, in particular, high cooling rates are generally expected to limit the extent of a chemical reaction since the reaction times available for the melt/reinforcement interfaces are significantly reduced (Ref 65). The result of EDX line analysis (Fig. 12) conducted in the near vicinity of Al-graphite interface, in case of MC-HPDC sample revealed the presence of segregation of silicon. Selected processing temperature range, a shorter cycle time of MC-HPDC process, a higher cooling rate in pressure die casting, and the presence of Si (8.54 wt.%) improve the performance in terms of production cost and good interfacial integrity between reinforcement and the matrix.

3.4 Mechanical Properties

The uniform distribution and the nature of the interfacial bonding between graphite particles and matrix have an important bearing on the mechanical properties of a composite material. It has been suggested that graphite particles, being very weak compared to the aluminum matrix, may be treated as non-load-bearing constituents (Ref 32). With a view to extending their applications to structural components, these materials should have a good combination of strength and ductility. Figure 13 shows a comparison of the mechanical properties of LM24/graphite composite samples produced by the two different processes. The MC-HPDC composites show an increase in the tensile elongation together with an increase in the ultimate tensile strength of the material, resulting from the better dispersion of the particles. The magnitudes of these increases are observed to average approximately 20%.

There have been a number of publications in the literature where mechanical properties of Al alloy-graphite composites

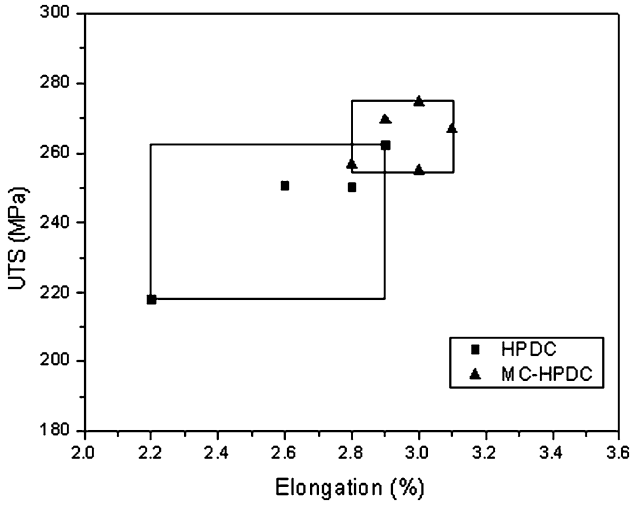

Fig. 13 Comparison of mechanical properties of LM24/graphite composites obtained from the two processes

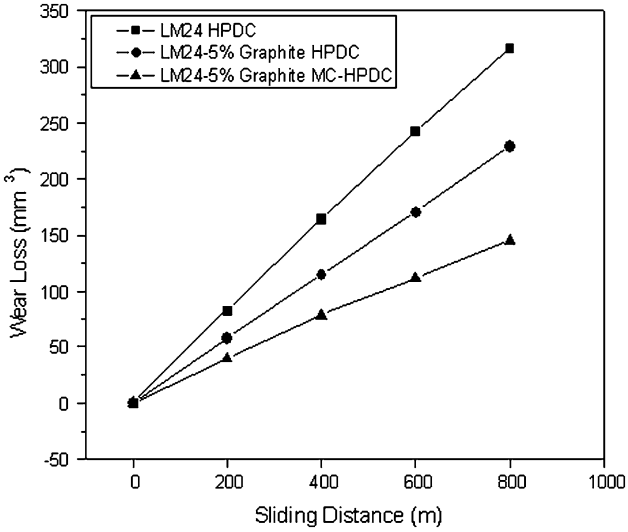

Fig. 14 Wear loss vs. sliding distance characteristics

Table 2 Normalized UTS data comparison

Matrix graphite composition, wt.%	Normalized UTS (σ_c/σ_m)	Reference
LM13-3graphite (die cast)	0.72	(Ref 66)
LM30-3graphite (die cast)	0.70	(Ref 66)
Al-11.8Si-1Mg-3graphite (as cast)	0.72	(Ref 67)
Al-12Si-1.5Mg-Cu-Ni-3graphite (gravity die cast)	0.77	(Ref 9)
LM13-3graphite (UPAL)	0.77	(Ref 21)
LM24-3.5graphite (HPDC)	0.83	Present study
LM24-3.5graphite (MC-HPDC)	0.90	Present study

are documented (Ref 9, 21, 33, 34, 41, 59, 60). However, different investigators have used different experimental procedures. In order to characterize the mechanical properties of Al alloy-graphite composites, the strengths have been normalized with respect to the base matrix. Table 2 shows the normalized UTS (UTS of composite, σ_c/UTS of matrix, σ_m) data from various investigations. The homogeneous distribution of graphite particles in MC-HPDC-processed composite samples, results in a reasonably high UTS value compared with the base alloy, which is in turn reflected in the high value of their normalized UTS.

A comparison of wear rate between an LM24 HPDC alloy and LM24-5% graphite composites is shown in Fig. 14. It can be seen that the wear loss of the matrix alloy and composites increased linearly with sliding distance. As expected, the high wear resistance of Al-graphite composites is primarily to due to the presence of graphite particles which act as a solid lubricant (Ref 11, 12, 15). Figure 15 revealed well-dispersed graphite particles on the worn surface of MC-HPDC composite which was processed at 620 °C, 120 s, and 800 rpm. The improved wear resistance of MC-HPDC composite is attributed to the uniform dispersion of graphite particles in the matrix. In view of these superior mechanical properties of Aluminum-graphite MC-HPDC composites compared with HPDC composites, they could be attractive candidates for automotive applications.

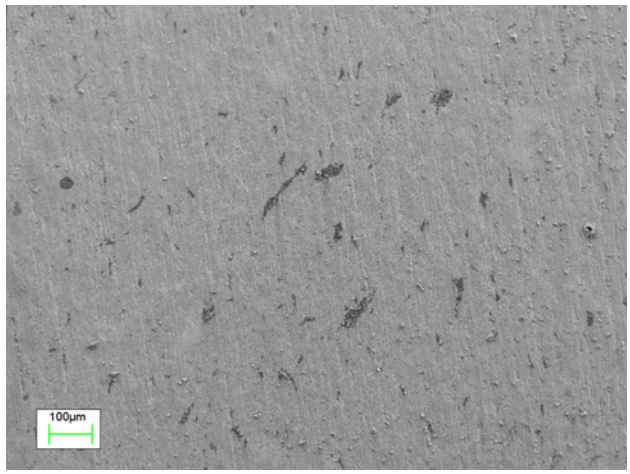

Fig. 15 SEM image of the worn surface of MC-HPDC sample

4. Conclusions

An efficient mixing technology to achieve a uniform distribution of uncoated graphite particles within an aluminum alloy matrix has been developed. The MC-HPDC process offers near-net shape components of high integrity. Quantitative image analysis revealed an improved particle distribution in the composite. The high dispersive shearing action and high intensity of turbulence created by the twin screws in the barrel lead to a uniform distribution of the reinforcement by overcoming the tensile strength of agglomerates. It was observed that prolonged shearing impairs the mixture quality. Quantitative analysis of the reinforcement distribution and mechanical properties confirmed the advantages of the MC-HPDC process over conventional processes. Improved mechanical properties are achieved due to structural uniformity and strong interfacial bonding.

Acknowledgment

The authors acknowledge the financial support from EPSRC.

References

1. K.K. Chawla, *Composite Materials*, 2nd ed., Springer, New York, 1998, p 3–5
2. T.W. Clyne and P.J. Withers, *An Introduction to Metal Matrix Composites*, 1st ed., Cambridge University Press, Cambridge, 1993, p 1–10
3. P. Rohatgi, Cast Metal Matrix Composites: Past, Present and Future, *AFS Trans.*, 2001, **109**, p 1–133
4. I.A. Ibrahim, F.A. Mohamed, and E.J. Lavernia, Particulate Reinforced Metal Matrix Composites—A Review, *J. Mater. Sci.*, 1991, **26**(5), p 1137–1156
5. S. Ray, Review Synthesis of Cast Metal Matrix Particulate Composites, *J. Mater. Sci.*, 1993, **28**(20), p 5397–5413
6. S.V. Prasad and R. Asthana, Aluminum Metal Matrix Composites for Automotive Applications: Tribological Considerations, *Tribol. Lett.*, 2004, **17**(3), p 445–453
7. B.P. Krishnan, N. Raman, K. Narayanaswamy, and P.K. Rohatgi, Performance of An Al-Si Graphite Particle Composite Piston in a Diesel Engine, *Wear*, 1980, **60**, p 205–215
8. S. Biswas, A. Shantharam, N.A.P. Rao, K. Narayana Swamy, P.K. Rohatgi, and S.K. Biswas, Bearing Performance of Graphitic Aluminum Particulate Composite Materials, *Tribol. Int.*, 1980, **13**, p 171–176
9. B.P. Krishnan, N. Raman, K. Narayanaswamy, and P.K. Rohatgi, Performance of Aluminum Alloy Graphite Bearings in a Diesel Engine, *Tribol. Int.*, 1983, **16**(5), p 239–244
10. S. Biswas and P.K. Rohatgi, Tribological Properties of Cast Graphitic-Aluminum Composites, *Tribol. Int.*, 1983, **16**(2), p 89–102
11. P.K. Rohatgi, S. Ray, and Y. Liu, Tribological Properties of Metal Matrix-Graphite Particle Composites, *Int. Mater. Rev.*, 1992, **37**(3), p 129–149
12. B.C. Pai, P.K. Rohatgi, and S. Venkatesh, Wear Resistance of Cast Graphitic Aluminum Alloys, *Wear*, 1974, **30**, p 117–125
13. P.R. Gibson, A.J. Clegg, and A.A. Das, Wear of Cast Al-Si Alloys Containing Graphite, *Wear*, 1984, **95**, p 193–198
14. F.A. Badia and P.K. Rohatgi, Gall Resistance of Cast Graphitic Aluminum Alloy, *SAE Trans.*, 1969, **78**, p 1200–1207
15. P.K. Rohatgi and B.C. Pai, Seizure Resistance of Cast Aluminum Alloys Containing Dispersed Graphite Particles of Various Sizes, *Wear*, 1980, **59**, p 323–332
16. J. Zhang, R.J. Perez, and E.J. Lavernia, Effect of SiC and Graphite Particulates on the Damping Behavior of Metal Matrix Composites, *Acta Metall. Mater.*, 1994, **42**(2), p 395–409
17. P.K. Rohatgi, D. Nath, S.S. Singh, and B.N. Keshavaram, Factors Affecting the Damping Capacity of Cast Aluminum-Matrix Composites, *J. Mater. Sci.*, 1994, **29**, p 5975–5984
18. H. Hocheng, S.B. Yen, T. Ishihara, and B.K. Yen, Fundamental Turning Characteristics of a Tribology-Favored Graphite/Aluminum Alloy Composite Material, *Compos. Part A: Appl. Sci. Manuf.*, 1997, **28**(9–10), p 883–890
19. P.K. Rohatgi, N. Murali, H.R. Shetty, and R. Chandrashekhar, Improved Damping Capacity and Machinability of Graphite Particle-Aluminum Alloy Composites, *Mater. Sci. Eng.*, 1976, **26**, p 115–122
20. B.C. Pai and P.K. Rohatgi, Production of Cast Aluminum-Graphite Particle Composites using a Pellet Method, *J. Mater. Sci.*, 1978, **13**(2), p 329–335
21. B.P. Krishnan, M.K. Surappa, and P.K. Rohatgi, The UPAL Process: A Direct Method of preparing Cast Aluminum Alloy-Graphite Particle Composites, *J. Mater. Sci.*, 1981, **16**(5), p 1209–1216
22. P.R. Gibson, A.J. Clegg, and A.A. Das, Production and Evaluation of Squeeze Cast Graphitic Al-Si Alloys, *Mater. Sci. Technol.*, 1985, **1**, p 559–567
23. B.K. Prasad, T.K. Dan, and P.K. Rohatgi, Characterization and Microstructural Modifications of a Pressure Die Cast Eutectic Aluminium-Silicon Alloy-Graphite Composite, *Mater. Trans. JIM*, 1993, **34**(5), p 474–480
24. F. Akhlaghi and S.A. Pelaseyyed, Characterization of Aluminum/Graphite Particulate Composites Synthesized using a Novel Method termed "In situ Powder Metallurgy", *Mater. Sci. Eng. A*, 2004, **385**, p 258–266
25. N. Eustathopoulos, J.C. Joud, P. Desre, and J.M. Hicter, The Wetting of Carbon by Aluminum and Aluminum Alloys, *J. Mater. Sci.*, 1974, **9**(8), p 1233–1242
26. K. Landry, S. Kalogeropoulou, and N. Eustathopoulos, Wettability of Carbon by Aluminum and Aluminum Alloys, *Mater. Sci. Eng. A*, 1998, **254**, p 99–111
27. D.M. Stefanescu, A. Moitra, A.S. Kacar, and B.K. Dhindaw, The influence of Buoyant Forces and Volume Fraction of Particles on the Particle Pushing/Entrapment Transition During Directional Solidification of Al/SiC and Al/Graphite Composites, *Metall. Trans. A*, 1990, **21**(1), p 231–239
28. R. Asthana, S. Das, T.K. Dan, and P.K. Rohatgi, Solidification of Aluminum-Silicon Alloy in the Presence of Graphite Particles, *J. Mater. Sci. Lett.*, 1986, **5**(11), p 1083–1086
29. T.P.D. Rajan, R.M. Pillai, and B.C. Pai, Reinforcement Coatings and Interfaces in Aluminium Metal Matrix Composites, *J. Mater. Sci.*, 1998, **33**(14), p 3491–3503
30. B.C. Pai, G. Ramani, R.M. Pillai, and K.G. Satyanarayana, Role of Magnesium in Cast Aluminium Alloy Matrix Composites, *J. Mater. Sci.*, 1995, **30**(8), p 1903–1911
31. C.S. Narendranath, P.K. Rohatgi, and A.H. Yegneswaran, Observation of Graphite Structure Under Optical and Scanning Electron Microscopes, *J. Mater. Sci. Lett.*, 1986, **5**(6), p 592–594
32. B.S. Majumdar, A.H. Yegneswaran, and P.K. Rohatgi, Strength and Fracture Behaviour of Metal Matrix Particulate Composites, *Mater. Sci. Eng.*, 1984, **68**, p 85–96
33. U.T.S. Pillai, R.K. Pandey, and P.K. Rohatgi, Effect of Volume Fraction and Size of Graphite Particulates on Fracture Behaviour of Al-Graphite Composites, *Eng. Fract. Mech.*, 1987, **28**(4), p 461–477
34. O.P. Modi, A.K. Singh, A.H. Yegneswaran, and P.K. Rohatgi, High-temperature Strength of an Aluminum Alloy Dispersed with Graphite Particles, *J. Mater. Sci. Lett.*, 1992, **11**(21), p 466–1468
35. G.J.C. Carpenter and S.H.J. Lo, Characterization of Graphite-Aluminum Composites using Analytical Electron Microscopy, *J. Mater. Sci.*, 1992, **27**(7), p 1827–1841
36. A.K. Jha, R. Asthana, T.K. Dan, and P.K. Rohatgi, Effect of Dispersed Graphite on the Freezing rate of Gravity Die-cast LM13 alloy-3 wt.% Graphite Particle Composite, *J. Mater. Sci. Lett.*, 1987, **6**(2), p 225–228
37. J.K. Kim and P.K. Rohatgi, Interaction between Moving Cellular Solidification Front and Graphite particles During Centrifugal Casting, *Mater. Sci. Eng. A*, 1998, **244**, p 168–177
38. S.W. Ip, R. Sridhar, J.M. Toguri, T.F. Stephenson, and A.E.M. Warner, Wettability of Nickel Coated Graphite by Aluminum, *Mater. Sci. Eng. A*, 1998, **244**, p 31–38
39. A. Sato and R. Mehrabian, Aluminum Matrix Composites: Fabrication and Properties, *Metall. Mater. Trans. B*, 1976, **7**(3), p 443–451
40. O.P. Modi, A.H. Yegneswaran, R. Asthana, and P.K. Rohatgi, Thermomechanical Processing of Aluminum-based Particulate Composites, *J. Mater. Sci.*, 1998, **23**(1), p 83–92
41. U.T.S. Pillai, B.C. Pai, K.G. Satyanarayana, and A.D. Damodaran, Fracture Behavior of Pressure Die-cast Aluminum-Graphite Composites, *J. Mater. Sci.*, 1995, **30**(6), p 1455–1461
42. U.T.S. Pillai, B.C. Pai, V.S. Kelukutty, and K.G. Satyanarayana, Pressure Die-cast Graphite Dispersed Al-Si-Mg Alloy Matrix Composites, *Mater. Sci. Eng. A*, 1993, **169**, p 93–98
43. B.K. Prasad, T.K. Dan, and P.K. Rohatgi, Pressure-induced Improvement in Interfacial Bonding between Graphite and the Aluminum Matrix in Graphitic-Aluminum Particle Composites, *J. Mater. Sci. Lett.*, 1987, **6**(9), p 1076–1078
44. Z. Fan, M.J. Bevis, and S. Ji, PCT Patent, WO 01/21343 A1, 1999
45. S. Ji, Z. Fan, and M.J. Bevis, Semi-solid Processing of Engineering Alloys by a Twin-Screw Rheomoulding Process, *Mater. Sci. Eng. A*, 2001, **299**, p 210–217
46. J. Pelleg, D. Ashkenazi, and M. Ganor, The Influence of a Third Element on the Interface Reactions in Metal-Matrix Composites (MMC): Al-Graphite System, *Mater. Sci. Eng. A*, 2000, **281**, p 239–247
47. T.A. Chernyshova and L.I. Kobeleva, Products of interaction in the Al-Si alloy-carbon fibre system, *J. Mater. Sci.*, 1985, **20**(10), p 3524–3528
48. N. Aniban, R.M. Pillai, and B.C. Pai, An analysis of impeller parameters for aluminium metal matrix composites synthesis, *Mater. Des.*, 2002, **23**, p 553–556
49. N. Harnby, M.F. Edward, and A.W. Nienow, *Mixing in the Process Industries*, 2nd ed., Butterworths-Heinemann Ltd., Oxford, 1985, 106 p
50. W. Beck, P. Forschner, R. Junghanns, D. Klatt, G. Philipp, F. Sauter, H. Schneider, T. Schneider, K.-H. Schwarzer, W. Schwechheimer,

R. Vettermann, and E. Zimmermann, *Handbook of Mixing Technology*, EKATO Ruhr- und Mischtechnik GmbH, Schopfheim, 1991, p RS1–RS10
51. H. Rumpf, *The Strength of Granules and Agglomerates, Agglomeration*, W.A. Knepper, Ed., Interscience Publishers, New York, 1962, p 379–418
52. K. Kendall, Agglomerate Strength, *Powder Metall.*, 1988, **31**(1), p 28–31
53. H. Tang, L.C. Wrobel, and Z. Fan, Fluid Flow Aspects of Twin-Screw Extruder Process: Numerical Simulations of TSE Rheomixing, *Model. Simul. Mater. Sci. Eng.*, 2003, **11**, p 771–790
54. P.A. Karnezis, G. Durrant, and B. Cantor, Characterization of Reinforcement Distribution in Cast Al-Alloys/SiC_p Composites, *Mater. Charact.*, 1998, **40**, p 97–109
55. R. Schouwenaars, V.H. Jacobo, and A. Ortiz, Quantitative Comparison of the Microstructural Quality of Two Classes of Commercial Soft Triboalloys, *Mater. Charact.*, 2008, **59**, p 312–320
56. J.T. Curtis and R.P. McIntosh, The Interrelations of Certain Analytic and Synthetic Phytosociological Characters, *Ecology*, 1950, **31**, p 434–455
57. A. Rogers, *Statistical Analysis of Spatial Dispersion: The Quadrat Method*, 3rd ed., Pion, London, 1974, p 1–164
58. Y.J. Lee, D.L. Feke, and I. Manas-Zloczower, Dispersion of Titanium Dioxide Agglomerates in Viscous Media, *Chem. Eng. Sci.*, 1993, **48**(19), p 3363–3372
59. C. Rauwendaal, *Polymer Extrusion*, 3rd Rev. ed., Hanser Publisher, New York, 1994, 181 p
60. M. Gupta, C. Lane, and E.J. Lavernia, Microstructure and Properties of Spray Atomized and Deposited Al-7Si/SiC_p Metal Matrix Composites, *Scr. Metall. Mater.*, 1992, **26**(5), p 825–830
61. P.K. Rohatgi, J. Sobczak, R. Asthana, and J.K. Kim, Inhomogeneities in Silicon Carbide Distribution in Stirred Liquids—a Water Model Study for Synthesis of Composites, *Mater. Sci. Eng. A*, 1998, **252**, p 98–108
62. A.P. Diwanji and I.W. Hall, Fibre and Fibre-Surface Treatment Effects in Carbon/Aluminium Metal Matrix Composites, *J. Mater. Sci.*, 1992, **27**(8), p 2093–2100
63. T. Etter, P. Schulz, M. Weber, J. Metz, M. Wimmler, J.F. Loffler, and P.J. Uggowitzer, Aluminium Carbide Formation in Interpenetrating Graphite/Aluminium Composites, *Mater. Sci. Eng. A*, 2007, **448**, p 1–6
64. B. Revzin, D. Fuks, and J. Pelleg, Influence of alloying on the solubility of carbon fibers in aluminium-based composites; Non empirical approach, *Compos. Sci. Technol.*, 1996, **56**, p 3–10
65. H.G. Seong, H.F. Lopez, D.P. Robertson, and P.K. Rohatgi, Interface Structure in Carbon and Graphite Fiber Reinforced 2014 Aluminum Alloy Processed with Active Fiber Cooling, *Mater. Sci. Eng. A*, 2008, **487**(1–2), p 201–209
66. S. Das, V. Prasad, and T.R. Ramachandran, Microstructure and Wear of Cast (Al-Si Alloy)-Graphite Composites, *Wear*, 1989, **133**, p 173–187
67. P.K. Rohatgi and M.K. Surappa, Deformation of Graphite during Hot Extrusion of Cast Aluminum-Silicon-Graphite Particle Composites, *Mater. Sci. Eng.*, 1984, **62**, p 159–162